Electronic Supplementary Material (ESI) for Journal of Materials Chemistry A.

S1. Electronic structure by GGA for PbI_2 termination

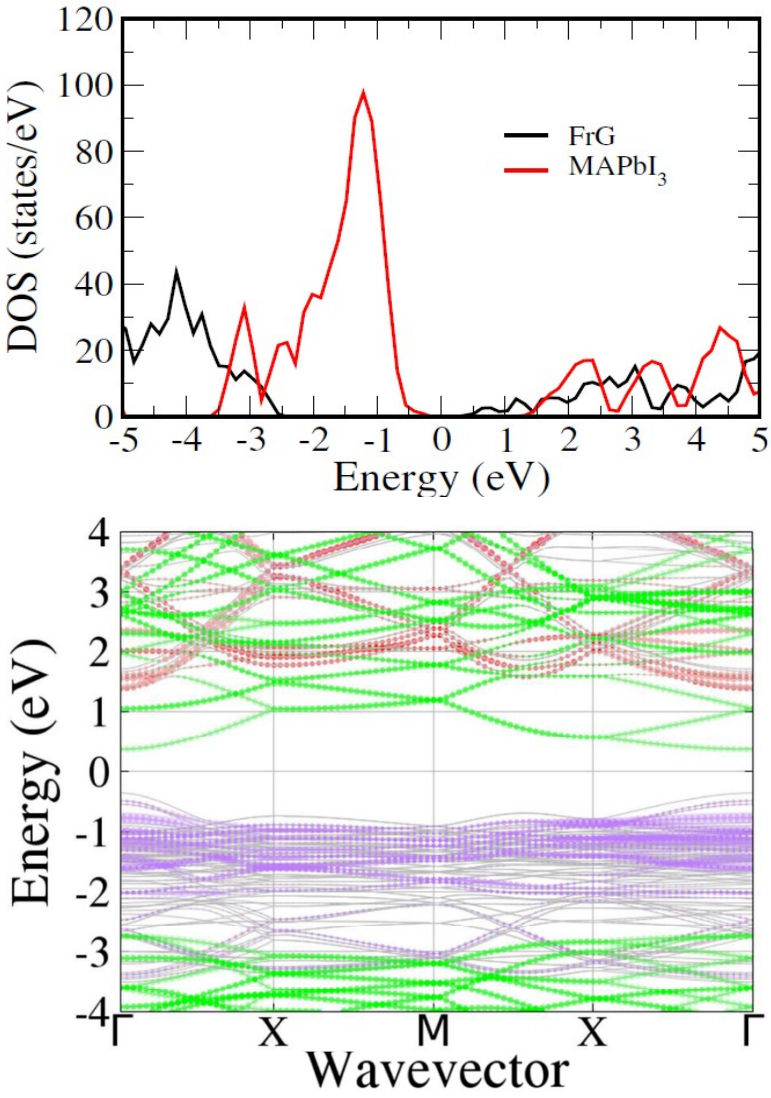

Figure S1. DOS (top) and electronic structure (bottom) calculated with GGA for PbI_2 termination. The color scheme for band structure plot: purple (I), red (Pb), green (FGr). The results are overall consistent with GGA+SOC calculation shown in main text (Fig. 2), though inclusion of SOC is necessary for reliable quantitative interpretation of the $MAPbI_3$ electronic structure.

S2. Electronic structure by GGA for MAI termination

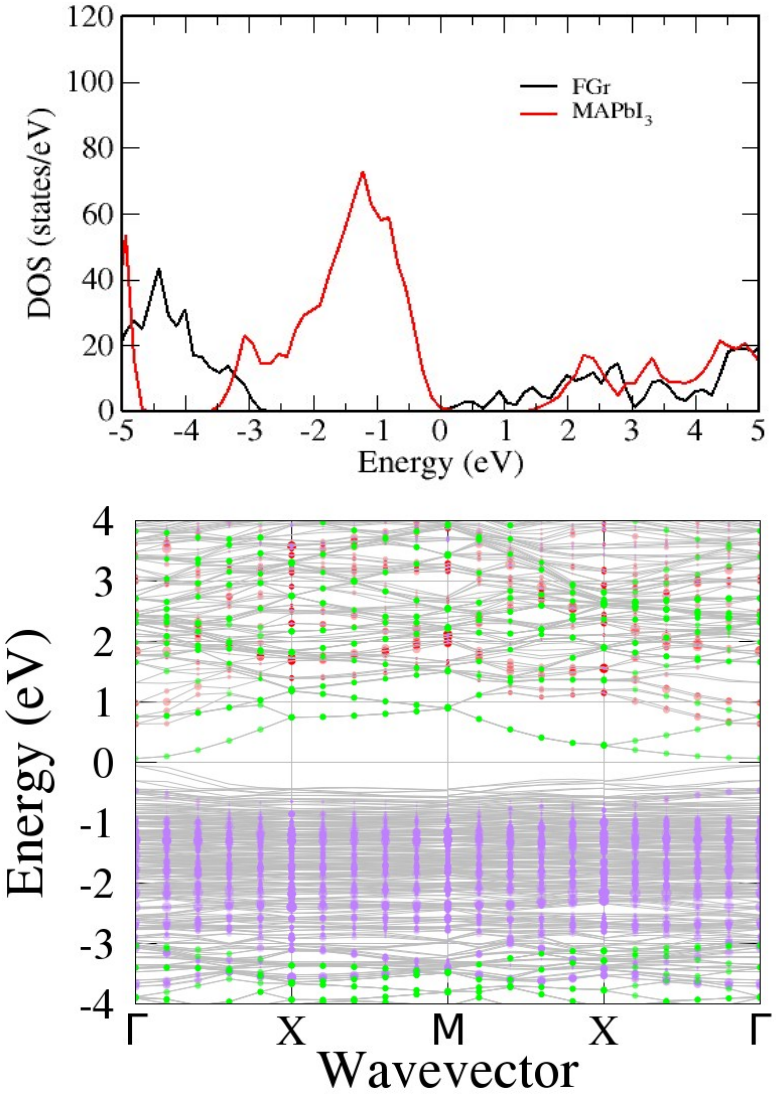

Figure S2. DOS (top) and electronic structure (bottom) calculated with GGA for MAI termination. The color scheme for band structure plot: purple (I), red (Pb), green (FGr).

S3. Correction of $MAPbI_3$ band gap

In order to correct the $MAPbI_3$ band gap for interface energy level diagrams, we performed fully self-consistent calculations for bulk $MAPbI_3$ using GGA+SOC as well as hybrid functionals, (HSE06+SOC and PBE0+SOC). We found a band gap of 0.46 eV for GGA+SOC which is underestimated by ~ 1eV in comparison to the experiments. Utilization of HSE06+SOC increased it only up to 0.9 eV.[2] On the other hand, PBE0+SOC provided a band gap of 1.40 eV, in much better agreement with the experimental value (1.5-1.6 eV).[3] Therefore, we have chosen PBE0+SOC method to correct energy level alignment for $MAPbI_3$ for FGr/$MAPbI_3$ interface.

Specifically, we compared the energy levels of $MAPbI_3$ as obtained from GGA+SOC and PBE0+SOC methods, referenced to average electrostatic potential obtained from each calculation. We found shifts of -0.64 (+0.30) for valence (conduction) bands. We note that these values are in line with previously results.[4] Finally, to test these results further, we also performed similar calculations for the $MAPbI_3$ slab employed in this work. This is important since due to presence of vacuum level, such shifts can be calculated without any ambiguity. Indeed, the comparison of energy levels (referenced to vacuum level for each method) provided the shifts of VBM/CBM for GGA and hybrid calculations, in good agreement with the method outlined above (differences were within 0.05 eV).

S4. Energy level alignment at FGr/TiO_2 interface

In order to directly ascertain the energy level alignment for FGr/TiO_2 interface, we compare the ionization potentials (positions of VBM with respect to vacuum) of individual FGr and TiO_2 slabs. This approach is reasonable since FGr is chemically inert so covalent interaction at the interface will be very weak. As a consequence, positions of VBM/CBM of FGr and TiO_2 at the interface should be similar to that of pristine slabs. As an example, here we use rutile (110) surface of TiO_2 whose ionization potential is ~7.83 eV as determined recently by a combined experimental/theoretical study,[5] whereas our calculations suggest an ionization potential of 7.81 eV for FGr. The energy level alignment is shown below (Fig. S3). The CBM of FGr is 0.1 eV higher in energy than that of TiO_2. Thus, the band alignment as obtained directly from FGr/TiO_2 interface clearly shows that charge transfer is facilitated at FGr/TiO_2 interface, in good agreement with results discussed in manuscript (Fig. 3, main text). We note that this conclusion is also valid for energetically favorable anatase (101) surface since its CBM is 0.2 eV lower than that of rutie (110) surface.[5]

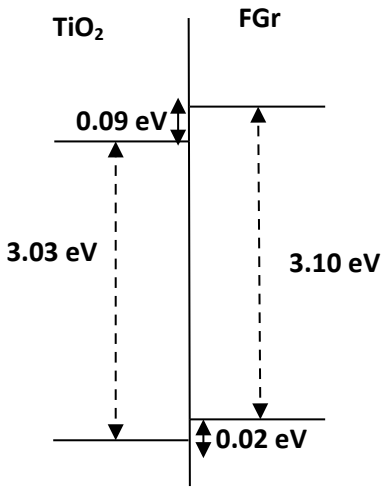

Fig S3: Energy level alignment at TiO_2/FGr interface. The ionization potential (position of VBM with respect to vacuum) of TiO_2 (FGr) is 7.83 eV (7.81 eV).

S5. Hydrophobicity of FGr as compared to graphene

The binding energies (E_b) ater molecule to graphene and FGr are calculated by using the methods of PBE+TS and PBE0+TS. The 3x3 graphene (or FGr) supercell is adopted with the enough vacuum size (> 14 Å), and the structural optimization is done with the atomic force criteria 0.02 eV/Å. Our optimized structures (top and side views) and the binding energy are shown in Fig. S4 for graphene (top) and FGr (bottom), where PBE+TS result is given first and PBE0+TS inside parentheses. From graphene to FGr, it shows a substantial decrease in binding energy.

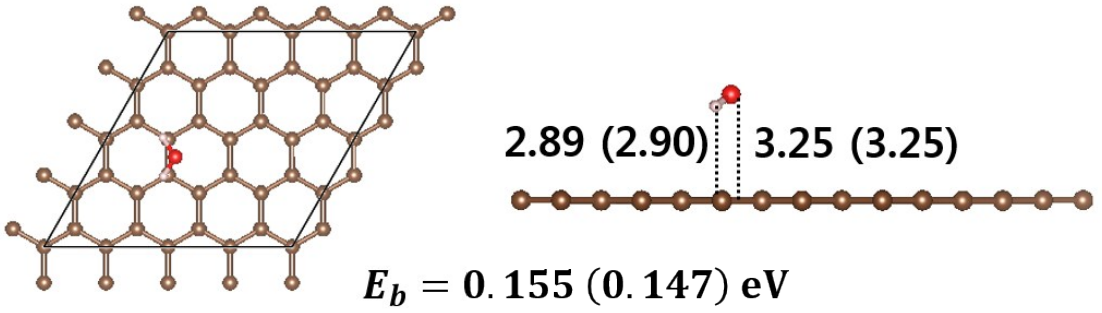

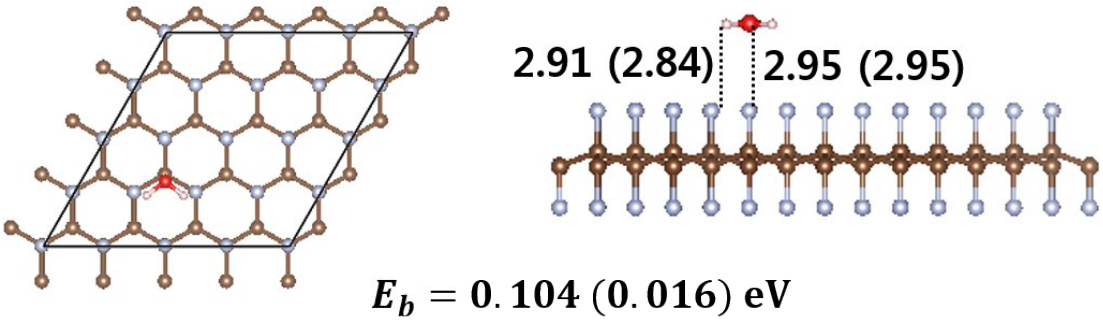

Fig S4: Optimized structures (in Å) and binding energies of a water molecule adsorbed on graphene (top) and FGr (bottom) at the PBE+TS (PBE0+TS) level of theory. The PBE0+TS values are in parentheses.

In order to calculate the contact angle, we carried out 5 ns MD simulations with the extended simple point charge model of water molecule on graphene (SPCE) and FGr at room temperature in NVT ensemble. The OPLS_AA force field is used for the interaction parameters. To measure the contact angle, we divide the entire simulation cell into cubic bins and calculate the local density of these bins separately.

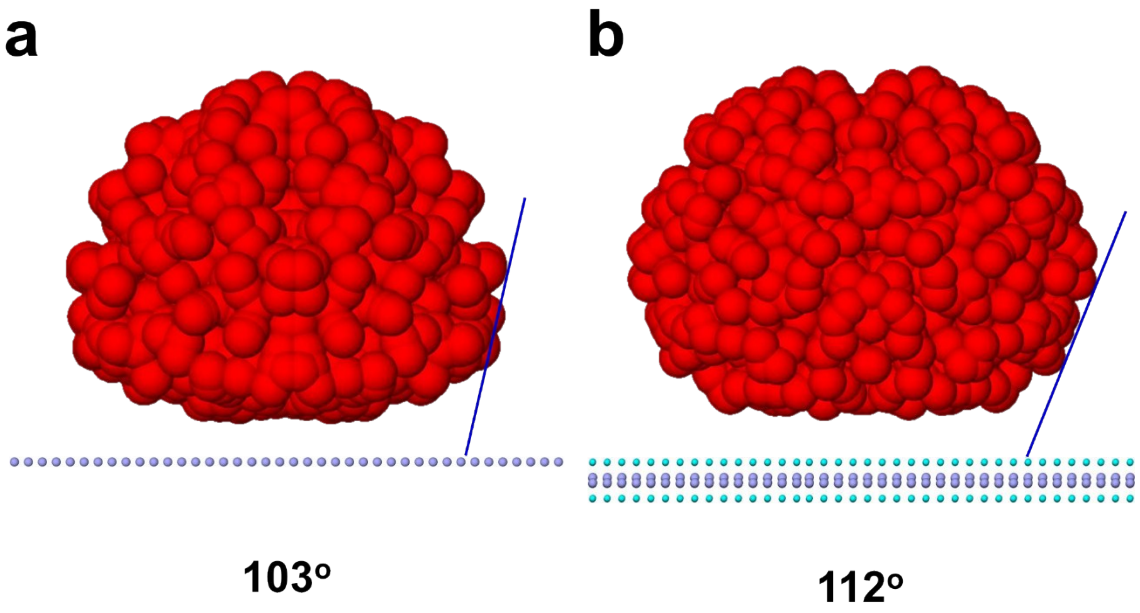

Fig S5: The contact angle of the water nano-droplet that includes 1,000 water molecules on graphene shows 103° (in good agreement with the experimental value[6] of 95-100°), while the value of 112° is obtained for this droplet on FGr. This clearly indicates that FGr is more hydrophobic than graphene.

S6. Electronic structure and energy level alignment for non-ferroelectric $MAPbI_3$ slab.

In order to see the impact of MA orientation on the energy level alignment, we performed additional calculations with non-polar symmetrical $MAPbI_3$ slab where dipole moments of neighboring MAI layers are orientated oppositely (Fig. S6, red arrows). The energy level diagram obtained from PBE0+SOC method is shown in Fig S6 (right). In comparison to the energy level alignment shown in main text (Fig. 3, corresponding slab in Fig. 1), conduction band offset is reduced slightly to ~ 0.36 eV. Nevertheless, electron transfer/hole blockage remains energetically favorable, consistent with the major finding discussed in the main text.

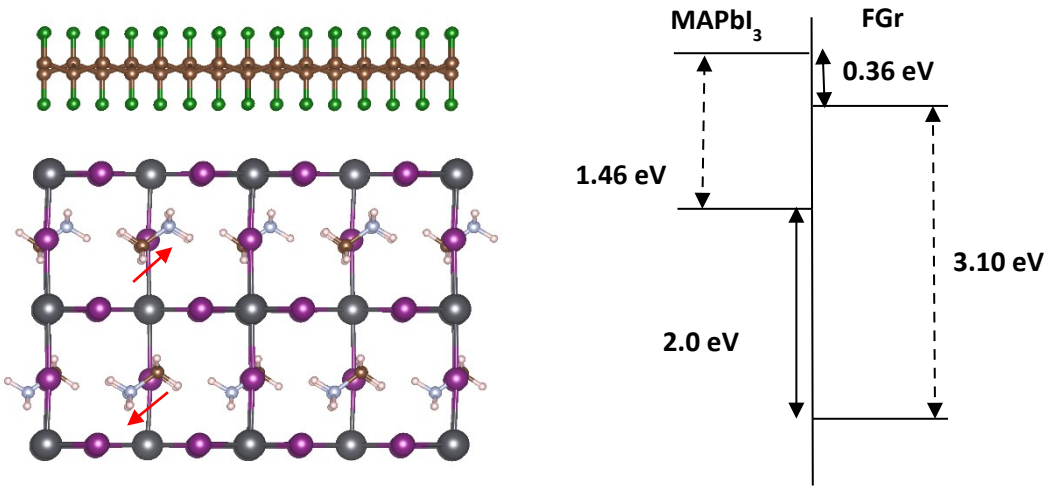

Fig S6: (Left) FGr/$MAPbI_3$ interface with non-polar $MAPbI_3$ slab. The color scheme for atoms is the same as given in main text, Fig. 1. The red arrows indicate the direction of MA dipoles which are oriented in opposite direction for neighboring MAI layers. (Right) Energy level alignment diagram calculated with PBE0+SOC method. Double dashed arrows represent the band gaps while solid double arrows highlight the band offsets.

References

[1] Etienne, T.; Mosconi, E.; De Angelis, F. Dynamical Origin of the Rashba Effect in Organohalide Lead Perovskites: A Key to Suppressed Carrier Recombination in Perovskite Solar Cells? J. Phys. Chem. Lett. 2016, 7, 1638−1645.

[2] Hendon, C. H.; Yang, R. X.; Burton, L. A.; Walsh, A. Assessment of polyanion (BF_4^- and PF_6^-) substitutions in hybrid halide perovskites . *J. Mater. Chem. A* **2015**, 3, 9067– 9070.

[3] Wang, Q.; Lyu, M.; Zhang, M.; Yun, J.-Ho; Wang, L. Halide perovskite materials for solar cells: a theoretical review. *J. Mater. Chem. A*, **2017**, 5, 902.

[4] Menéndez-Proupin, E.; Palacios, P.; Wahnón, P.; Conesa, J. C. Self-consistent Relativistic Band Structure of the $CH_3NH_3PbI_3$ Perovskite. *Phys. Rev. B: Condens. Matter Mater. Phys.* **2014**, 90, 045207.

[5] D. O. Scanlon, C.W. Dunnill, J. Buckeridge, S. A. Shevlin, A. J. Logsdail, S. M.Woodley, C. R. A. Catlow, M.. J. Powell, R. G. Palgrave, I. P. Parkin, G. W. Watson, T. W. Keal, P. Sherwood, A.Walsh and A. A. Sokol1, Band alignment of rutile and anatase TiO_2. *Nat. Materials*, **2013**, 12, 798–801.

[6] C.-J. Shih, Q. H. Wang, S. Lin, K.-C. Park, Z. Jin, M. S. Strano, and D. Blankschtein, Breakdown in the Wetting Transparency of Graphene. *Phys. Rev. Lett.* **2012**, 109, 176101.